International Journal of Control and Automation
Vol.9, No.2 (2016), pp.383-394
http://dx.doi.org/10.14257/ijca.2016.9.2.36

Particle Swarm Optimization Applied to Generalized Predictive Control of a Solar Power Plant

Xiao-juan Lu[1], Hai-ying Dong[1] and Duo-jin Fan[2]

School of Automation and Electrical Engineering,
Lanzhou Jiaotong University, Lanzhou 730070, China1
National Engineering Technology Research Center of Green coating Technology and Equipment (Lanzhou Jiaotong University), Lanzhou 730070, China2
luxj@mail.lzjtu.cn, hydong@mail.lzjtu.cn, fanduojin1@sohu.com

Abstract

In this paper, generalized predictive control based on particle swarm optimization (PSO-GPC) was applied to the control of linear Fresnel distributed collector system, of which the purpose was to reduce the system error in the dynamic process. The main goal of solar thermal power generation system control was to control the collector outlet temperature in a certain range. Using the the rate of heat transfer oil in heat collector as input, outlet temperature as output and solar radiation intensity as a disturbance signal, model of Controlled Auto-Regressive Integrated Moving Average(CARIMA) was established. The control task of generalized predictive control (GPC) was to make the actual outlet temperature of systems as close as possible to the desired output trajectory. Gradient optimization without constraints was used to obtain the optimal control input, and gradient optimization with constraints and PSO optimization were matched with each other. A multi-mode hybrid optimization method was formed, which can obtain the optimal control increment of system quickly and accurately. GPC and PSO-GPC technology was applied to Lanzhou 200kW linear Fresnel solar thermal power generation demonstration system. Through the simulation results obtained from actual data we can see that the PSO-GPC control technology can reduce the error of the system dynamic process compared to GPC control technology.

Keywords*: Solar power plant, Linear Fresnel collector, generalized predictive control, Particle swarm optimization*

1. Introduction

Linear Fresnel thermal power generation system consists of light focusing and heat collecting subsystem, heat exchange subsystem, generating subsystem and heat storage subsystem. Light focusing and heat collecting subsystem are the core of the system. The solar radiation is focused into the linear Fresnel collector, then heat conducting oil in the heat collector is heated, which can convert solar energy into heat energy. Heat exchange subsystem is composed of super heater and evaporator, whose function is that using the high temperature heat transfer oil heated by the heat collector condenser to heat the water to generate high-temperature steam driving generator. When the solar radiation is strong, heat storage subsystem will store excess energy. When the solar radiation is insufficient or there is no solar radiation, using the thermal energy in heat storage subsystem heats the heat transfer oil cyclically to heat water and generate steam to drive the generator for power generation [1].

At present, solar thermal power generation system in China is still under development.

ISSN: 2005-4297 IJCA

The efficiency of solar energy is low and the cost of solar power generation is high, so the introduction of any kinds of advanced control technology will improve the efficiency of the system and also will promote the solar energy to replace traditional energy sources. A lot of articles have studied the solar field control algorithms which were used to realize the desired outlet-temperature where the water flow rate was the manipulated variable. Because of some factors these systems are not easy to control. For a solar distributed collector field the measurable external disturbances are difficult to deal with, so self-tuning proportional-integral controller based on a pole-assignment approach employing serial compensation was presented [2]. In order to track an outlet temperature a feedback linearization technique was used to manipulate the fluid flow rate through the solar field, and the effect of disturbances were weakened [3].

Generalized predictive controllers are also used to the distributed collector field of a solar power plant. Neural predictors obtained from the general identification methodology are used in a nonlinear predictive control scheme derived from the generalized predictive controller (GPC) structure [4, 5]. A special subclass of fuzzy inference systems used in the distributed collector field of a solar power plant, the TP (triangular partition) and TPE (triangular partition with evenly spaced midpoints) systems, can obtain adequate control signals in the whole range of possible operating conditions[6]. Non-linear optimal feedforward control of solar collector plants is not easy because of non-linear disturbance effects and long input-dependent transport delay. So as to obtain an accurate model of feedforward controller design, measured data were used in a black-box recursive prediction error identification algorithm. Accurate feedforward control was obtained in the simulation [7]. Making the outlet oil temperature to track a reference signal by manipulating the oil flow was included in the objective considered in the possible presence of fast disturbances caused by passing clouds, and in this process the plant was assumed to be a "black box" lumped parameter system[8]. The plant dynamics also can be approximated by an affine state-space neural network, of which the complexity is depend on the cardinality of dominant singular values associated with a subspace oblique projection of data-driven Hankel matrix [9]. The use of Nonlinear Model Predictive Controller (NMPC) can manipulate the oil flow rate to maintain the field outlet temperature in the desired reference value and attenuate the disturbances effects [10]. The application of a Nonlinear Model Predictive Controller (NMPC) extended with a dead-time compensator (DTC) of a distributed solar collector field also obtained good performance [11]. Model Predictive control algorithms for solar plants are very helpful to reject disturbances, but some conditions must be suitable for locality. Adaptive model predictive control using an unscented Kalman filter (UKF) was presented [12]. The results of above research literature were applied in the Acurex trough solar thermal power generation system in Spain. The final control goal of these documents is to make temperature of system output oil follow the desired value with minimum error.

The main control objective of solar thermal power generation system is to make outlet oil temperature of distributed solar heat collector maintain at a desired range, use solar radiation to heat the heat transfer oil, regulate the flow rate of the heat transfer oil, and control outlet temperature in a certain range. The control task of GPC is to make the actual output of the system as close as possible to the desired output trajectory, use PSO to find the optimal predictive control law and set the desired output and then apply feedback correction to correct the desired output prediction value [13, 14].

Based on the above analysis, this paper presents the PSO-GPC algorithm which was applied to the control of linear Fresnel collector system. This method used the following error of outlet temperature of heat collector as objective and applied the actual data to analyze. GPC algorithm and PSO-GPC algorithm were separately used to be compared, and the hybrid optimization algorithm can significantly reduce the following error and accelerate the convergence speed of the system. So it can ensure stationarity of solar thermal power generation system.

This paper is structured as follows: Section 2 is devoted to solar thermal power generation system description, section 3 is the derivation of CARIMA of distributed solar heat collecting system, and section 4 is the structure analysis of GPC algorithm and PSO-GPC algorithm and controller, section 5 is the contrast analysis of experiments. Finally, this paper make the analysis and comparison of two kinds of control algorithm application and plant results.

2. Solar Thermal Power Generation System

Thermal power generation system built in Lanzhou New District came online in 2012. Area of collector field is 2335m^2, photo-thermal conversion efficiency of system is 60%, the tracking precision of system is about 0.1°and construction area is 4000 m^2. The heat transfer medium of system is heat conducting oil, of which working temperature is 350℃. Using the oil-water heat exchange technology to get the steam whose temperature is 300 ℃ to drive the generator to generate electricity. The system is shown in Figure 1. Focusing system used linear Fresnel collector, of which the width is 16m and the length is 96m. Fresnel uses two times of condenser, the length of pipeline of heat transfer oil is L=220m and generator selects screw generator. Working process of the linear Fresnel thermal power generation system: Linear Fresnel condenser heats the heat transfer oil, the heat collecting pipe through the heat exchange subsystem heats water and generate steam, high temperature steam drives generator, the heat conduction oil through heat exchange subsystem enters the heat storage system and heat the heat storage salt to store heat and the heat conducting oil flowing out from thermal energy storage system after the circulation enters into linear Fresnel collector system. The Fresnel heat collecting part is shown in figure 2. Boiler pressure of screw expansion of power unit is 1.0Mpa; Exhaust pressure is 0.14Mpa; Continuous flow is 6.6 t/h; Power generation is 200kW; The annual power generation is 1.6 million kW·H.

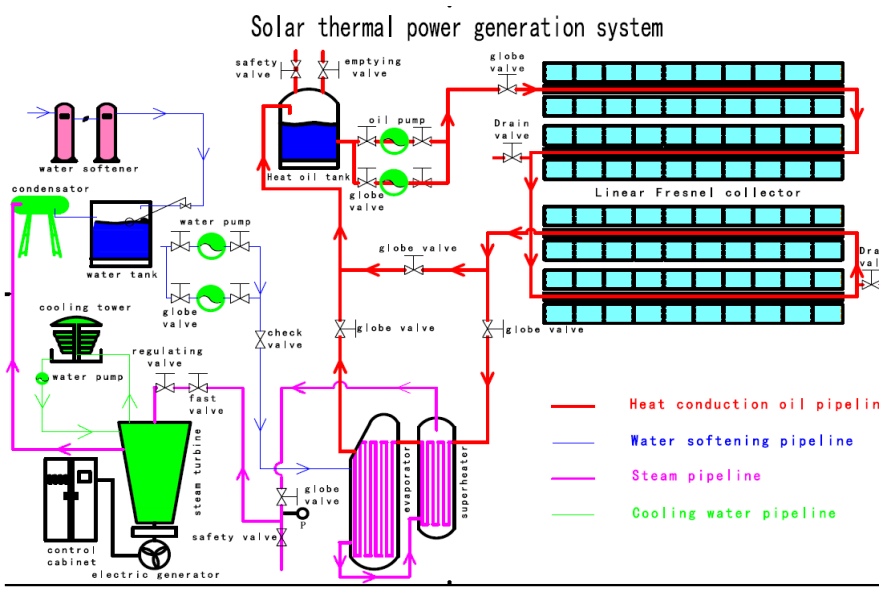

Figure 1. Structure of Linear Fresnel Thermal Power Generation System

Figure 2. Tracking Picture of Linear Fresnel Collector

3. Plant Model of Solar Thermal Power Generation

In 1985, the Spanish scholar Carmona, R. Initially used a distributed parameter model about temperature to describe the heat change of solar collector field in his doctoral thesis. He divided the tube length into a plurality of Δx and constructed a distributed parameter model which was expressed by partial differential equation (1) and (2). The control variable of control system is flow rate of the heat conducting oil. The output signal is outlet temperature of collector field. Interference signal is the actual measured solar radiation intensity. The model was used as the control model by scholars to simulate and analyze the control performance of the heat collecting system [6, 9, 15].

$$\rho_m C_m A_m \frac{\partial T_m}{\partial t} = \eta_0 GI(t) - h_l(T_m(x,t) - T_a(t)) - D\pi h_t(T_m(x,t) - T_f(x,t)) \quad (1)$$

$$\rho_f C_f A_f \frac{\partial T_f}{\partial t}(x,t) + \rho_f C_f u(t) \frac{\partial T_f}{\partial x}(x,t) = D\pi h_t(T_m(x,t) - T_f(x,t)) \quad (2)$$

where m represents metal and f represents fluid. All of the variables description is represented in table 1.

Table 1. Solar Power Plant Model Variables and Parameters

symbol	description	units
t	Time	s
x	Space	m
ρ	Density	kg m^{-3}
C	Specific heat capacity	JK^{-1}kg^{-1}
A	Cross-sectional area	m^2
$T(t,x)$	Temperature	K, ^{o}C
$u(t)$	Oil pump volumetric flow rate	m^{3}s^{-1}
$I(t)$	Solar irradiance	W m^{-2}
η_0	Mirror optical efficiency	
G	Mirror optical aperture	m
$T_{a(t)}$	Ambient temperature	K, ^{o}C
h_l	Global coefficient of thermal losses	W m^{-2} $^{o}C^{-1}$
h_t	Coefficient of metal-fluid transmission	W m^{-2} $^{o}C^{-1}$
D_i	Inner diameter of pipe line	m
L	Tube length	m

In formula (1) and (2), if we ignore the heat loss of metal and heat loss of heat transfer process, we can get formula (3).

$$\rho_f C_f A_f \frac{\partial T_f}{\partial t}(x,t) + \rho_f C_f u(t) \frac{\partial T_f}{\partial x}(x,t) = \eta_0 GI(t) \quad (3)$$

The formula (3) can be expressed by equation (4).

$$\rho_f C_f A_f \frac{dT_n(t)}{dt} = \eta_0 GI - \rho_f C_f u(t) \frac{T_n(t) - T_{n-1}(t)}{\Delta x} \qquad n = 1...N \quad (4)$$

Δx is the measured length of oil-way in the length range of Δx. $T_n(t)$ is oil outlet temperature of collector tube, $T_{n-1}(t)$ is inlet temperature and t is the time. While $\Delta x = L$ and L is the total length of collector tube, equation (4) can be expressed by equation (5).

$$\rho_f C_f A_f \frac{dT_n(t)}{dt} = \eta_0 GI(t) - \rho_f C_f u(t) \frac{T_n(t) - T_{n-1}(t)}{L} \qquad n = 1...N \quad (5)$$

$T_n(t)$、$T_{n-1}(t)$ are respectively the oil outlet temperature and the inlet temperature of collector tube, and t is the time.

According to the measured actual data and in the condition of big radiation intensity and good performance of heat storage, the variation range of outlet temperature and the inlet temperature is $20^\circ C \sim 25^\circ C$ at the same time under the action of reservoir oil between heat storage system and heat collecting system. When formula (5) is discrete and the sampling period is T, the equation (5) can be expressed by equation (6), in which $a = [T_n(t) - T_0(t)] / L$, $y(t) = T_n(t)$.

$$\rho_f C_f A_f \frac{[y(k+1)T] - y(kT)}{T} = \eta_0 GI(k) - \rho_f C_f au(k) \quad (6)$$

In which, $u(t)$ is input, $y(t)$ is output, $I(t)$ is disturbance, T is sampling period. The equation (6) can be expressed by equation(7).

$$y(k+1) = y(k) - \frac{T}{\rho_f C_f A_f} \times a \times u(k) + \frac{\eta_0 GT}{\rho_f C_f A_f} \times I(k) \quad (7)$$

Distributed Solar Collector (DSC) is a system of strong interference, of which heat transfer oil flow of the heat collector is input and oil outlet temperature is output. The intensity of solar radiation which can be measured actually is a disturbance signal. The equation (7) is the CARIMA model of system.

4. Controller Design

4.1. GPC Algorithm

The essence of generalized predictive control is optimization control algorithm that is to seek $\Delta u(k)$, $\Delta u(k+1)$, …… $\Delta u(k+N-1)$ when the objective function reaches the minimum value. Predictive control includes the model prediction, rolling optimization, feedback correction [13][16].

GPC algorithm based on CARIMA model is as follows. The CARIMA model can be expressed as(8).

$$\mathrm{A}(z^{-1}) y(k) = z^{-d} \mathrm{B}(z^{-1}) \Delta u(k) + \mathrm{C}(z^{-1}) \xi(k) \quad (8)$$

Where, $y(k)$、$\Delta u(k)$ and $\xi(k)$ are output, control increment and white noise respectively. d is the pure delay.

And

$$\begin{cases} \mathrm{A}(z^{-1}) = 1 + \mathrm{a}_{1,1} z^{-1} + \mathrm{a}_{1,2} z^{-2} + \cdots + \mathrm{a}_{1,\mathrm{n_a}} z^{-\mathrm{n_a}} \\ \mathrm{B}(z^{-1}) = \mathrm{b}_{1,0} + \mathrm{b}_{1,1} z^{-1} + \mathrm{b}_{1,2} z^{-2} + \cdots + \mathrm{b}_{1,\mathrm{n_b}} z^{-\mathrm{n_b}} \quad , \quad l_{1,0} \neq 0 \\ \mathrm{C}(z^{-1}) = 1 + \mathrm{c}_{1,1} z^{-1} + \mathrm{c}_{1,2} z^{-2} + \cdots + \mathrm{c}_{1,\mathrm{n_c}} z^{-\mathrm{n_c}} \end{cases} \tag{9}$$

According to the formula(9), minimum variance of output prediction model of system in the future time is expressed by formula(10).

$$\mathbf{Y}^* = \mathbf{Y}_\mathrm{m} + \mathbf{G}\Delta\mathbf{U} \tag{10}$$

$\mathbf{Y}_\mathrm{m}$ is the past output of system. $\mathbf{Y}^*$ is predict output in future.

$$\mathbf{Y}^* = \left[y^*(k+d \mid k),\ y^*(k+d+1 \mid k), \cdots, y^*(k+N \mid k) \right]^T \tag{11}$$

$$\mathbf{Y}_\mathrm{m} = [y_\mathrm{m}(k+d), y_\mathrm{m}(k+d-1), \cdots, y_\mathrm{m}(k+N)]^T \tag{12}$$

$$\Delta\mathbf{U} = [\Delta u(k), \Delta u(k+1), \cdots, \Delta u(k+N-d)]^T \tag{13}$$

$$\Delta u(k+i) = u(k+i) - u(k+i-1)\,, i = 0\,,1\,,\cdots, N-d \tag{14}$$

$$\mathbf{G} = \begin{bmatrix} b_{1,0} & 0 & \cdots & 0 \\ b_{2,0} & b_{1,0} & \cdots & 0 \\ \vdots & \vdots & & \vdots \\ b_{N-\mathrm{d}+1,0} & b_{N-\mathrm{d},0} & \cdots & b_{1,0} \end{bmatrix}_{(N-\mathrm{d}-1)\times(N-\mathrm{d}-1)} \tag{15}$$

G is the control matrix.

In formula (12) $y_\mathrm{m}(k+j)$ is determined by input and output of the past, which can be obtained from (16).

$$\begin{aligned} y_\mathrm{m}(k+j) = &-\sum_{i=1}^{n_a} \mathrm{a}_{1,\mathrm{i}} y_\mathrm{m}(k+j-i) + \sum_{i=0}^{n_b} \mathrm{b}_{1,\mathrm{i}} \Delta u(k+j-d-i \mid k) \\ &+ \sum_{i=0}^{n_c} \mathrm{c}_{1,\mathrm{i}} \xi(k+j-i \mid k)\,, \qquad j = 1\,,2\,,\cdots N \end{aligned} \tag{16}$$

In which

$$\Delta u(k+i \mid k) = \begin{cases} 0\,, i \geq 0 \\ \Delta u(k+i)\,, i < 0 \end{cases}$$

$$\xi(k+i \mid k) = \begin{cases} 0\,, i \geq 0 \\ \xi(k+i)\,, i \leq 0 \end{cases}$$

$$y_m(k+i) = y(k+i), i \leq 0$$

Matrix element of formula (15) can be obtained from (17).

$$b_{\mathrm{j},0} = b_{1,\mathrm{j}-1} - \sum_{i=1}^{j_1} a_{1,\mathrm{i}} b_{\mathrm{j}-\mathrm{i},0} \qquad j = 2\,,3\,,\cdots, N-d+1 \tag{17}$$

In which $j_1 = \min\{j-1, n_a\}$; while $j-1 > n_b$, $b_{1,j-1} = 0$.

$$\begin{cases} y_r(k+d-1) = y_m(k+d-1) \\ y_r(k+d+i) = \alpha y_r(k+d+i-1) + (1-\alpha)\omega(k+d) \quad , i = 0,1,\cdots, N-d \\ \mathbf{Y}_r = \left[y_r(k+d), y_r(k+d+1), \cdots y_r(k+N) \right]^T \end{cases} \tag{18}$$

$\omega(k)$ is the desired output of k moment. α is soft output coefficient. $\mathbf{Y}_r$ is reference trajectory vector. The minimized objective function is expressed by (19).

$$J = E\left\{ (\mathbf{Y} - \mathbf{Y}_j)^T (\mathbf{Y} - \mathbf{Y}_r) + \Delta \mathbf{U}^T \mathbf{\Gamma} \Delta \mathbf{U} \right\} \tag{19}$$

Corresponding generalized predictive control is as follows.

$$\Delta \mathbf{U} = (\mathbf{G}^T \mathbf{G} + \mathbf{\Gamma})^{-1} \mathbf{G}^T (\mathbf{Y}_r - \mathbf{Y}_m) \tag{20}$$

So control variable at the moment can be obtained .

$$u(k) = u(k-1) + \Delta u(k) = u(k-1) + [1,0,\cdots 0](\mathbf{G}^T \mathbf{G} + \Gamma)^{-1} \mathbf{G}^T (\mathbf{Y}_r - \mathbf{Y}_m) \tag{21}$$

$\mathbf{\Gamma}$, unit matrix, is the control weighting matrix. To sum up, the GPC control struc- ture is shown in figure 3.

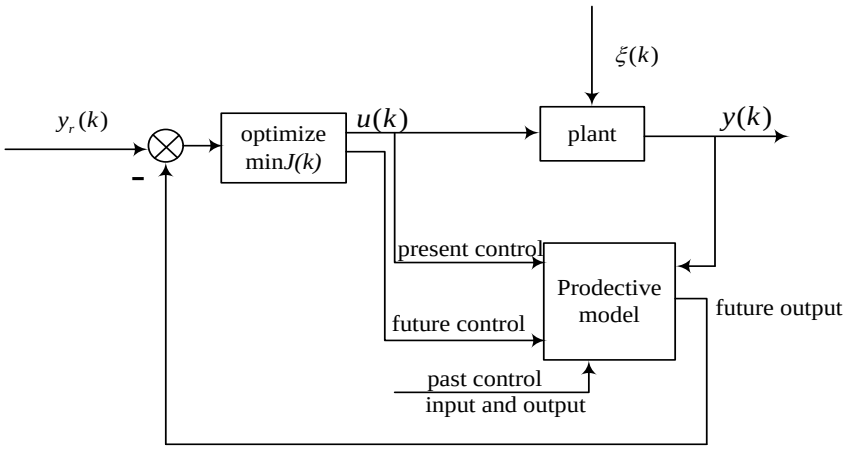

Figure 3. GPC Control Structure

4.2. PSO-GPC Algorithm

In 2007, generalized predictive algorithm optimized by particle swarm has been studied and some simple applications of simulation have been performed.

4.2.1 PSO algorithm

Particle swarm optimization algorithm [17-19] is described as follows: If the dimension of search space is n, the population consists of m particles, $x = (x_1, x_2, \cdots, x_m)^T$ and $x_i = (x_{i,1}, x_{i,2} \cdots x_{i,n})^T$ is the position of particle i ,velocity of which is $v_i = (v_{i,1}, v_{i,2} \cdots v_{i,n})^T$. Individual extreme of the particle is $p_i = (p_{i,1}, p_{i,2} \cdots p_{i,n})^T$, and the global extreme of the population is $p_g = (p_{g,1}, p_{g,2} \cdots p_{g,n})^T$. When particles find individual and global extreme, they update the velocity and position according to the following

two formula.

$$v_{i,d}^{k+1} = v_{i,d}^{k} + c_1 r_1 (p_{i,d}^{k} - x_{i,d}^{k}) + c_2 r_2 (p_{g,d}^{k} - x_{i,d}^{k}) \quad (22)$$

$$x_{i,d}^{k+1} = x_{i,d}^{k} + v_{i,d}^{k} \quad (23)$$

Where c_1 and c_2 are weight coefficient of acceleration, r_1 and r_2 are random function between (0, 1), $v_{i,d}^{k}$ and $x_{i,d}^{k}$ are respectively the velocity and position of d dimension of particle i in the K iteration. $p_{i,d}^{k}$ Is the position of Individual extreme of d dimension of particle i. $p_{g,d}^{k}$ Is the position of global extreme of d dimension of population.

According to the evolution Equations of particles above, c_1 regulate the step which can make particle fly to the best position of itself and c_2 regulate the step which can make particle fly to the best position of overall situation. At the same time in order to reduce the possibility in the evolutionary process of particles leaving the search space, $v_{i,d}$ is usually restricted in a certain range $v_{i,d} \in [-v_{\max}, v_{\max}]$. If the search space of question is restricted in $[-x_{\max}, x_{\max}]$, $v_{\max}$ can be set $v_{\max} = kx_{\max}$, $0 \le k \le 1$.

4.2.2 PSO-GPC Algorithm

According to the performance index (19), the essence of the optimization problem is the optimization problem with constraints. The traditional optimization methods are difficult to solve, so we use the PSO algorithm to optimize the performance index (19) and then solve the predictive control law directly. Specific steps are as follows.

The performance index (19) can be seen as fitness function of the PSO algorithm, and the parameters to be optimized of PSO algorithm are $\Delta u(k+j-1|k), j=1,...,N$ which are amount of change sequence of predictive control variable. The range of parameters optimization is $[\Delta u_{\min}, \Delta u_{\max}]$. There are N parameters to be optimized, Then the dimension of parameter space of PSO algorithm is $D=N$. The position of j particle can be expressed as a as a vector whose dimension is N that is $X_j = [\Delta u_j(k|k), \Delta u_j(k+1|k), ...\Delta u_j(k+N-1|k)], j=1,...,M$. Each element are iteratively updated through formula (21), and then optimal performance index (19) is calculated. If the performance indexes meet the end condition, the position of the particle whose fitness function value is minimum in particle swarm is the optimal predictive control sequence. The first element is the control input at current time in the system, and the next moment repeat the above process. So we can get the optimal control.

$$u^*(k) = u^*(k-1) + \Delta u^*(k) \quad (24)$$

5. Simulation Analysis

According to the actual operation data, when the outlet temperature reached above150 ℃, system began producing power. The control range of the oil outlet temperature is 160℃~220℃. The range of oil flow is 3l/s~12l/s. The sampling period is $T = 20\text{s}$. At the same time, temperature difference of oil outlet temperature and the inlet temperature is 25 ℃. $\rho_f = 800\text{kg/m}^3$, $C_f = 2600J/kg\cdot^\circ C$, $A_f = 0.65\text{m}^2$ η_0 =0.60 ; $G = 0.8\text{m}$, $L = 220\text{m}$. Simulation results are shown as below.

The data of June 9, 2014 and June 19th respectively were used to make simulation research. GPC algorithm and PSO-GPC algorithm were used to make simulation analysis.

The simulation results are in figure 4 to figure 11. In the figures, OBJECT denotes the set future output target curve $y_r(k)$; GPC represents the simulation results of GPC technology; And PSO-GPC represents the simulation results of PSO-GPC technology.

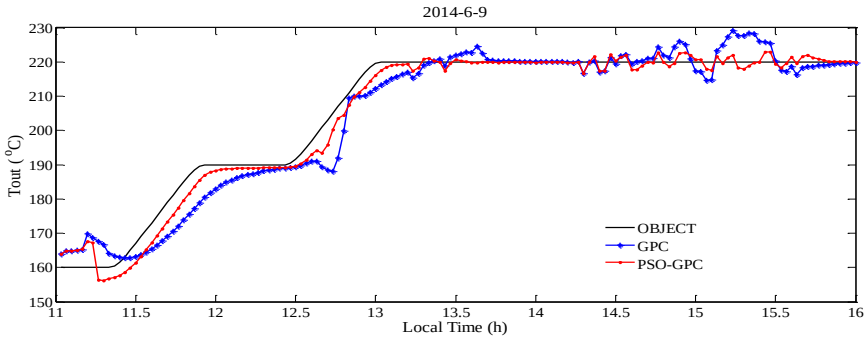

Figure 4. 6-9 Comparison of the Results of Oil Outlet Temperature

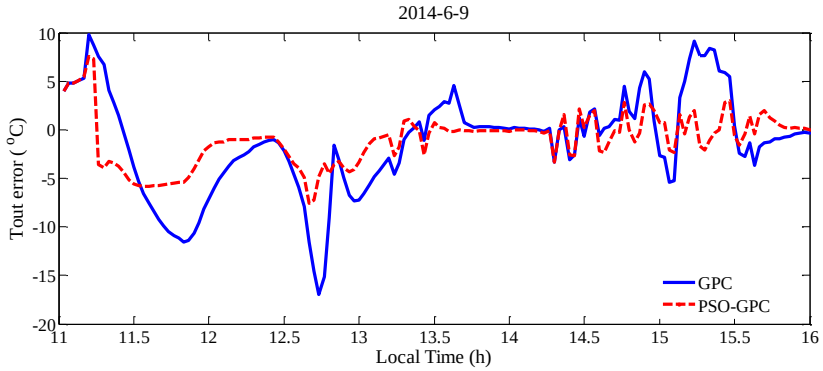

Figure 5. 6-9 Comparison of the Results of Output Error

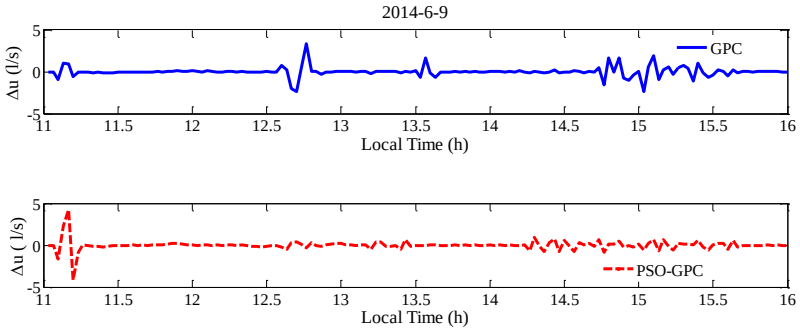

Figure 6. 6-9 Comparison of the Results of Control Increment after Optimization

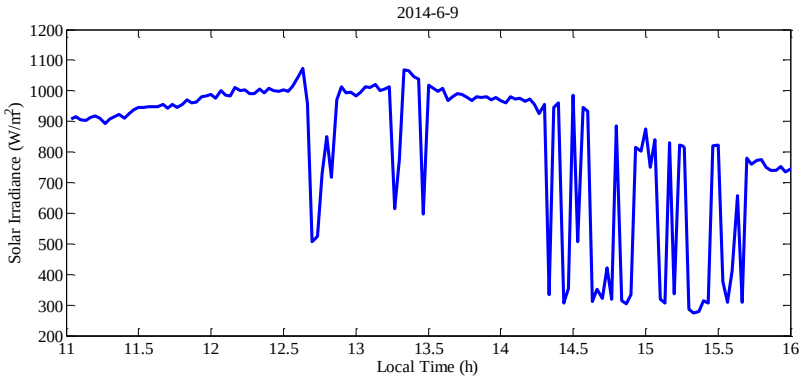

Figure 7. 6-9 the Actual Measured Solar Radiation

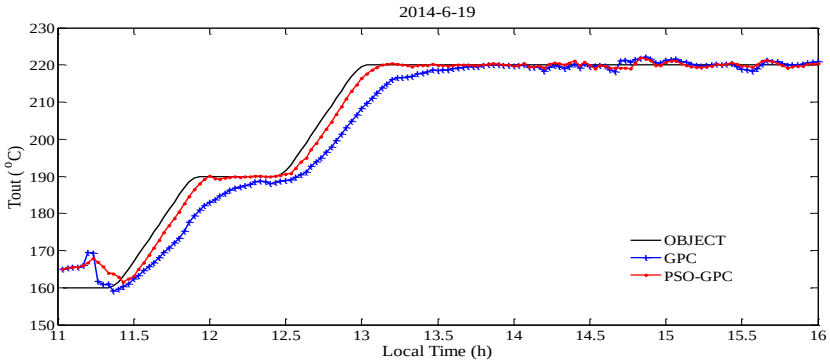

Figure 8. 6-19 Comparison of the Results of Oil Outlet Temperature

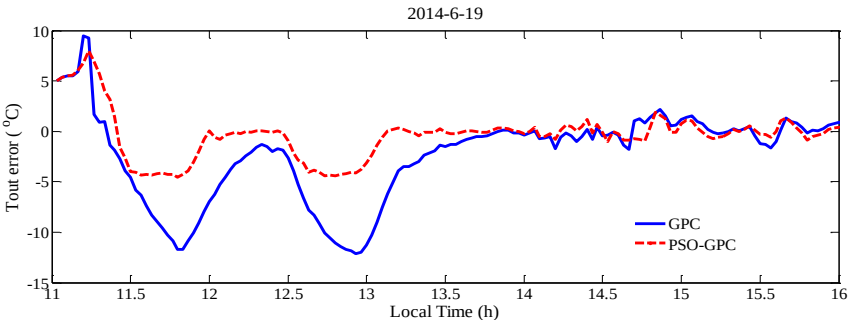

Figure 9. 6-19 Comparison of the Results of Output Error

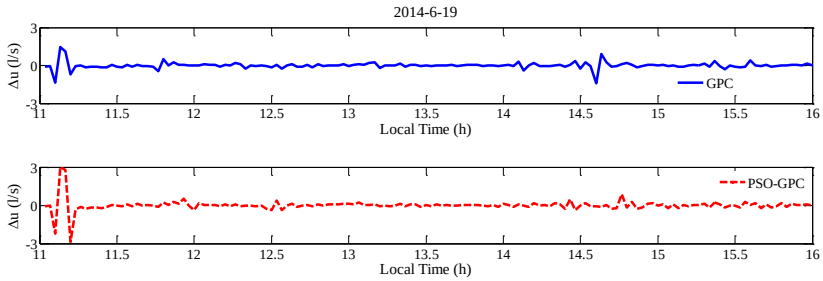

Figure 10. 6-19 Comparison of the Results of Control Increment after Optimization

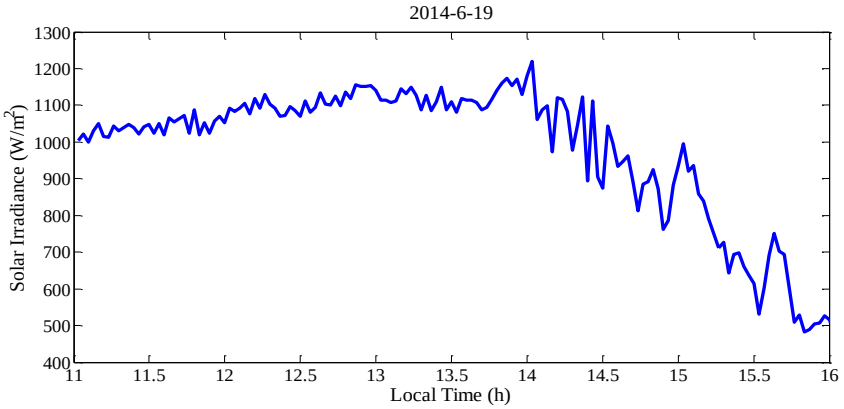

Figure 11. 6-19 the Actual Measured Solar Radiation

As can be seen from the above simulation results, the sun radiation of June 9th is large which had big fluctuations after 14:00 pm. but to raise to 800 W/m^2. The highest output temperature of oil outlet temperature is set at 220℃. When the working temperature of screw generator reached 150℃, it will start working. Therefore, a part of the heat of solar radiation was used for power generation part, and another part of the heat can be used as storage. So power generation and heat storage can be done at the same time.

Through using the actual data of two days, application of GPC algorithm used into control of linear Fresnel collector system was verified effective. When added hybrid particle swarm optimization algorithm, control effect was improved. As can be seen from the results of optimization of two algorithm storage and generating state. After 13:30 pm of June 19th the solar radiation decreased slowly. After 15:30 pm solar radiation is reduced to below 600W/m^2, at this point the oil outlet temperature was rely on heat storage system to heat transfer oil. After 16:00 pm if solar radiation did not rebound, the oil outlet temperature is difficult to maintain at 220℃. It can be seen from the two days' control simulation results that output error of hybrid optimization is smaller when hybrid optimization is added. Therefore hybrid optimization had better control effect. PSO-GPC reduced the system output error and stabilized the incremental change of control variable relatively. The range of output error of June 9th is -17℃~10℃ and the range of output error of June 19th is -13℃~9℃. After using the hybrid optimization algorithm, the range of output error of June 9th is -7℃~7℃and the range of output error of June 19th is -4℃~7℃. After 13:00 pm the output error of hybrid optimization became small. After about 14:20 pm of June 9th the solar radiation had fluctuations, but it can rise to 800 W/m^2. So the system has been running in the heat

6. Conclusion

This paper deduced and established the CARIMA model of Linear Fresnel solar thermal power generation system and applied PSO-GPC control algorithm into control of solar thermal power generation system. GPC and PSO-GPC control algorithm were both applied to Lanzhou Dacheng Fresnel thermal power generation system. The actual data was used to simulate, verify and analyze. In terms of comparison of GPC and PSO-GPC algorithm, PSO- GPC algorithm decreases the system output error and the amplitude variation of the temperature. Therefore, the PSO-GPC algorithm was applied to the control of linear Fresnel collector system effectively.

Acknowledgements

This work was supported by the National High Technology Research and Development Program of China (863 Program, No.2013AA050401) and the Gansu Provincial Natural Science Foundation of China granted by 1208RJZA180.

References

[1] S.Y. Huang and S.H. Huang, "Principle and Technology of Solar Thermal Power Generation", China electric power press, Bei Jing, **(2012).**
[2] E.F. Camacho, F.R Rubioa and F.M. Hughes, "Self-tuning control of a solar power plant with a distributed collector field", Journal of IEEE Control Systems Magazine, vol. 12, no. 2, **(1992)**.
[3] C.M. Cirre, L. Valenzuela, M. Berenguel and E.F. Camacho, "Feedback linearization control for a distributed solar collector field. J.Control Engineering Practice, vol. 15, no. 12, **(2007)**.
[4] E.F. Camacho and M. Berenguel, "Application of generalized predictive control to a solar power plant", In: Proceedings of the EC Esprit/CIM CIDIC Conferences on Advances in Model-Based Predictive Control, **(1994)**, Oxford, UK.
[5] E.F Camacho, M. Berrnguel and F.R. Rubio, "Application of a gain scheduling generalized predictive controller to a solar power plant", Journal of Control Practice, vol. 2, no. 2, **(1994)**.
[6] F.R. Rubio, M. Berenguel and E.F. Camacho, "Fuzzy logic control of a solar power plant", Fuzzy Systems，J.IEEE Transactions, vol. 3, no. 4, **(1995)**.
[7] L. Brus, T. Wigren and D. Zambrano, "Feedforward model predictive control of a non-linear solar collector plant with varying delays", Journa IET Control Theory and Applications, vol. 4, no. 8, **(2010)**.
[8] R.N. Silva, J.M. Lemos and L.M. Rato, "Variable sampling adaptive control of a distributed collector solar field", Journal of Control Systems Technology, IEEE Transactions, vol. 11, no. 5, **(2003)**.
[9] P. Gil, J. Henriques, A. Cardoso, P. Carvalho and Dourado, "Affine Neural Network-Based Predictive Control Applied to a Distributed Solar Collector A. Field", J. Control Systems Technology, IEEE Transactions, vol. 22, no. 2, **(2014)**.
[10] G.A. Andrade, D.J. Pagano, J.D. Álvarez and M. Berenguel, "A practical NMPC with robustness of stability applied to distributed solar power plants", J. Solar Energy, vol. 92, **(2013)**.
[11] M. Gá, l. Carrillo, R. De Keyser and C. Ionescu, "Nonlinear predictive control with dead-time compensator: Application to a solar power plant", J. Solar Energy, vol. 83, no. 5, **(2009)**.
[12] A.J. Gallego and E.F. Camacho, "Adaptative state-space model predictive control of a parabolic-trough field", J. Control Engineering Practice, vol. 20, no. 9, **(2012)**.
[13] E.F. Camacho and C. Bordons, "Model Based Predictive Control", Springer, **(2004)**.
[14] Y.G. Xi and D.W. Li, "Fundamental philosophy and status of qualitative synthesis of model predictive control", J. Acta Automatica Sinica, vol. 34, no. 10, **(2008)**.
[15] R. Carmona, "Analysis, Modeling and Control of a Distributed Solar Collector Field with a One-Axis Tracking System", University of Seville, **(1985)**, Spain.
[16] D.F. He, B.C. Ding and S.Y. Yu, "Review of fundamental properties and topics of model predictive control for nonlinear systems", J. Control Theory & Applications, vol. 30, no. 3**, (2013)**.
[17] B.X. Xiao, Z.G. Zhu and Y.F. Liu, "Research of Hybrid Optimized Generalized Predictive Controller Based on Particle Swarm Optimization", J. Journal of System Simulation, vol. 19, no. 4, **(2007)**.
[18] N. Dong, Z.Q. Chen, Q.L. Sun and Z.Z. Yuan, "Particle-swarm optimization algorithm for model predictive control with constraints", Journal of Control Theory & Application, vol. 26, no. 9, **(2009)**.
[19] S.T. Guan, J.Z. Chu and S. Shao, "Application of nonlinear model predictive control based on particle swarm optimization", Journal of Beijing university of chemical industry, vol. 34, no. 6**, (2007)**.

